

Deep Foundation Numerical Analysis Using Modified Compression Modulus

Hussein Yousif Aziz* and Jianlin Ma

School of Civil Engineering, Southwest Jiaotong University, Chengdu, Sichuan 610031, China,

Abstract: This paper is a study on the behavior and prediction of settlement values of bridge pile foundations due to construction loads. Field test results show new field technique using the single point of account settlement meter to estimate the thickness of compressed layer in the deep soft soils which is considered as a difficult task in the field. The settlement is predicted using hyperbolic model and statistical regression. The statistical models indicate that the structure would remain safe for a long period of time, and the field measurements are compared with the hyperbolic model results and those predicted by the statistical regression. The finite element Plaxis 3D Foundation program is used in the analysis with a new empirical equation to modify the input parameters represented by the soil compression modulus. The foundation soils are modeled with the Mohr-Coulomb plasticity material model. The piles are represented with pile elements, between the pile and the surrounding soil, interface elements are automatically generated by the program. In the analysis, the effects due to soil stiffness, pile length and pile spacing are considered. The calculated results for the simulation of the pile installation sequence are compared with the measured results obtained from the field monitoring. The results of the numerical analysis using the proposed empirical equation provide insight to the settlement analysis of pile groups in soft clayey soils and the finite element Plaxis 3D program can be a useful tool for numerical analysis. In this paper, the numerical analysis calculations are modified using a new empirical equation to calculate the compression modulus from those obtained from the test which modify the results of the settlement and thus become close to the reality. Finally, the numerical finite element analysis produced logical and conservative results as compared to the statistically derived equations and those calculated by hyperbolic model analysis. This scenario can be applied to the similar problems in the theoretical applications of bridge foundations.

Keywords: Compression modulus, 3D finite elements, hyperbolic model, settlement monitoring, soil plasticity, statistical regression.

1. INTRODUCTION

Bridges account for 80.4% of the total length of the Beijing-Shanghai high-speed railway in its northeast plain. Bored piles are commonly used in bridge rail tracks with a ballast-free form. Most of the railway paths from Beijing to Jinan city run over deep soft soil. The majority of the northern Shanghai sections to Danyang run over deep soft soil with a high water content, high compressibility, low intensity, poor permeability and long duration of consolidation deformation. Bridge foundation settlement control and prediction have become a key technical difficulty in these sections of the project. The bridges' stability is dependent on the strict control of the settlement process. The bridge is designed to support a speed of 350 kilometres per hour, with an initial speed of 300 kilometres per hour. At the same time, it must support the cross-line operation speed of the train, which is a minimum of 200 kilometres per hour.

In bridge engineering, settlement (including absolute settlement and differential settlement) of pile-group foundation is an important index reflecting construction safety and

quality [1]. Calculation methods of settlement adopted by most of the criteria are usually conservative and theory basis which are scant and deficient [2]. FEM is one of the most practical methods to predict the behavior of foundations. For pile foundation, however, due to the difficulty in evaluating the interaction of pile-soil-pile system and the behavior of excess pore water pressure, quantitative prediction method for long-term settlement in soft ground soil still needs to be improved [3]. For performance-based design of pile foundations, it is necessary to develop a practical prediction method for long-term displacements of pile foundation. There are a number of prediction methods for the settlement in soft ground [4, 5 and 6]. Current methods of settlement calculations show different advantages and disadvantages [7].

In this paper, the new monitoring technique by a single point of settlement level meter is used to measure the settlement in the deep soft soil. Calculation and prediction of pile group foundation settlement still needs research. The statistical models are used to predict the settlement of the deep soft soils in the project using the hyperbolic model and statistical regression. The literature reviewing on the subject of compression modulus adopts a theme which has relation with the soil stress [8, 9]. Authors have proposed an empirical equation to calculate the compression modulus depending on the depth of the soil layers. The calculations of three-

*Address correspondence to this author at the Southwest Jiaotong University, Chengdu, Sichuan-China; Tel: 008615002842434; E-mail: husseinyousif_9@yahoo.com; husseinyousif3@hotmail.com

dimensional Plaxis Foundation program are modified to conduct a numerical analysis that simulated the vertical displacement of the soil and other parameters to adjust the values of compression modulus obtained from the test, and getting precious results close to the reality. The other finding is to estimate the thickness of the compressed layer using the single point of settlement level meter which is considered as a difficult task in the field.

2. EXPERIMENTAL

2.1. Joint Monitoring Principle of Single-Point Settlement Gauge and Liquid Level Settlement Gauge

Single-point settlement gauge consists of anchor end, length rod and sensor. Anchoring both sides of length rod, with a sensor in the middle, to pile-top and certain soil to measure the total amount of soil compression. Its working principle is based on electromagnetic induction; a magnetized cylinder rod is fixed to the length rod which can move back and forth in coil. The coil inductance value is corresponding to the length of the rod in coil, the coil inductance value varies by length rod displacement, and then the inductance value transforms into frequency signal and displays in the reading device. Automatic data collection and remote transmission of single-point gauge are achieved through joint detection of automatic remote monitor system and single-point settlement gauge.

Liquid level settlement gauge consists of hydraulic cylinder, float, precise liquid level gauge, protection cover and other components. The survey point of liquid level settlement gauge is installed on cushion cap and its datum mark is installed on soil layer without disturbing the group pile foundation, which is used to measure the settlement of pile-

top. Its working principle is: tracheal tube connected by fluid, the liquid in the hydraulic cylinder is always in the same horizontal plane, when settlement occurs to the survey point, the liquid level sensor value increases (the difference value is positive), meanwhile, the liquid level sensor value in datum mark decreases (the difference value is negative). Automatic data collection and remote transmission of liquid level settlement gauge are achieved through joint detection of automatic remote monitor system and liquid level settlement gauge. Joint monitor of single-point settlement gauge and liquid level settlement gauge are shown in Fig. (1).

Certain pile soil compression value d is measured by single-point settlement gauge, cushion cap settlement s is measured by liquid level settlement gauge, and the settlement of cushion cap and settlement of pile-top are the same. The certain soil layer settlement value can be derived from subtracting the compression value of single-point settlement gauge from the settlement value of liquid level settlement gauge, which is $s - d$. Generally, compression value d and settlement s have the following relation $s \geq d$. Joint monitor calculation principle is shown in Fig. (2).

When the foundation is sinking, the settlement sheet with basic equipment goes down. Connectivity level settlement as shown in Fig. (3) is an intelligent digital inductance bus-type displacement meter FM, settlement is level difference measuring point – benchmark level difference.

Automatic composite measuring system is a powerful, fully automatic and static data collecting system which consists of host computer, acquisition module (MCU), system software components and related accessories (see Figs. 4 and 5). Field acquisition module (MCU) can be connected with string-type sensor (consists of strain gage, stress gage, pres-

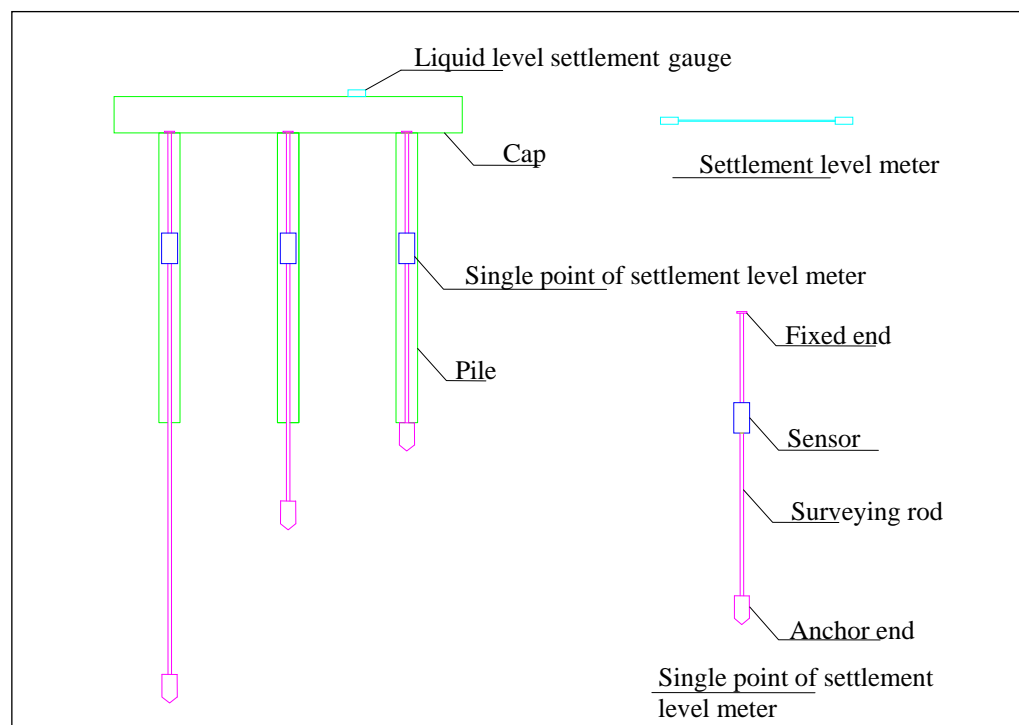


Fig. (1). Single settlement meter and level meter schematic joint monitoring.

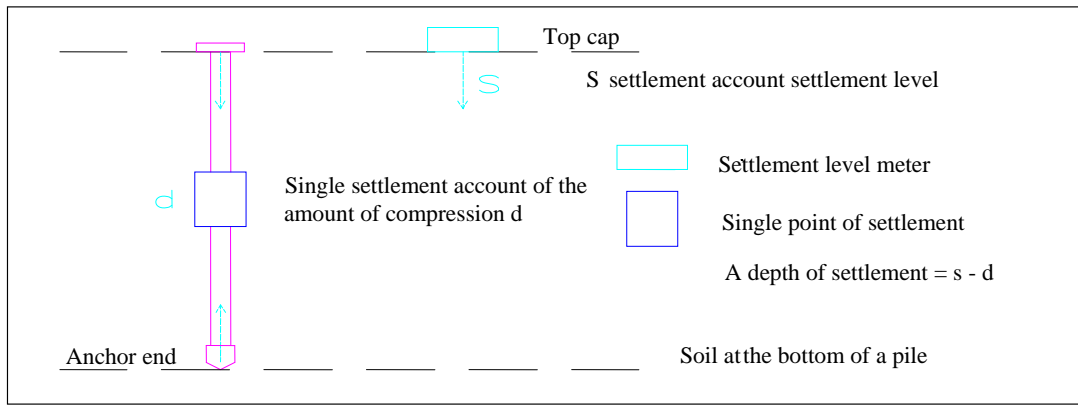


Fig. (2). A characteristic curve diagram of pile soil settlement calculation.

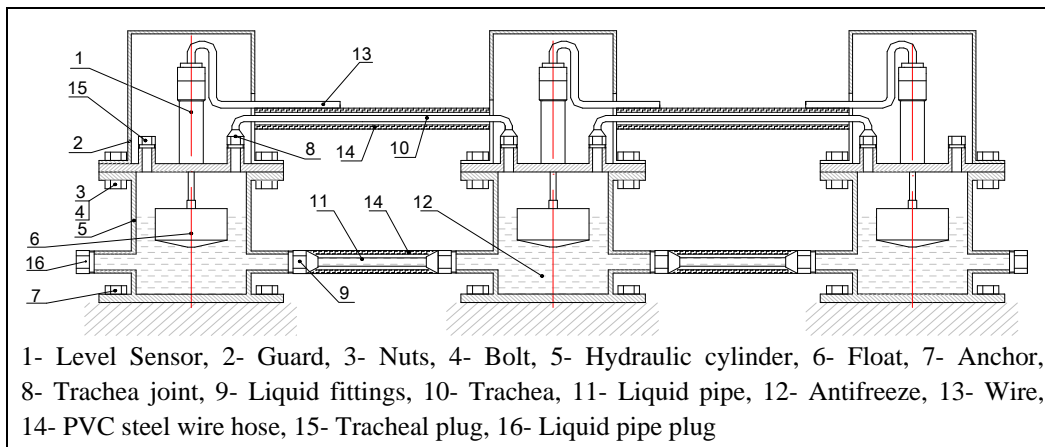


Fig. (3). Embedded connectivity of settlement level diagram.

sure cell, ohmmeter, cable meter, load sensor etc.), inductive frequency-modulation type sensor (consists of universal displacement meter, crack meter and rock change level meter etc.), bus-type sensor (consists of static force water level gauge, a bus cable tension gauge etc.), semiconductor or thermostat temperature sensor, resistance strain type sensor and standard voltage signal sensor. The system is designed as fully sealed, waterproof, and anti-lightning. Its distributed structure can compose 8~2000 points in measurement system. Through the measurement system real time data collec-

tion and remote wireless transmit function of single-point settlement gauge and liquid level settlement gauge can be achieved.

2.2. Bridge Foundation Model

Fig. (6.A) shows that the bridge foundation is a pile foundation located at DK124 worksite for piers D18 and D19 with cap dimensions of 12.5×9.1 m and stepped capping thicknesses of 2.5 m and 1.5 m. The number of piles is 12 bored piles with a diameter of 1.25 m; the spacing between



Fig. (4). Automatic remote monitor system.



Fig. (5). Connected settlement liquid level settlement gauge.

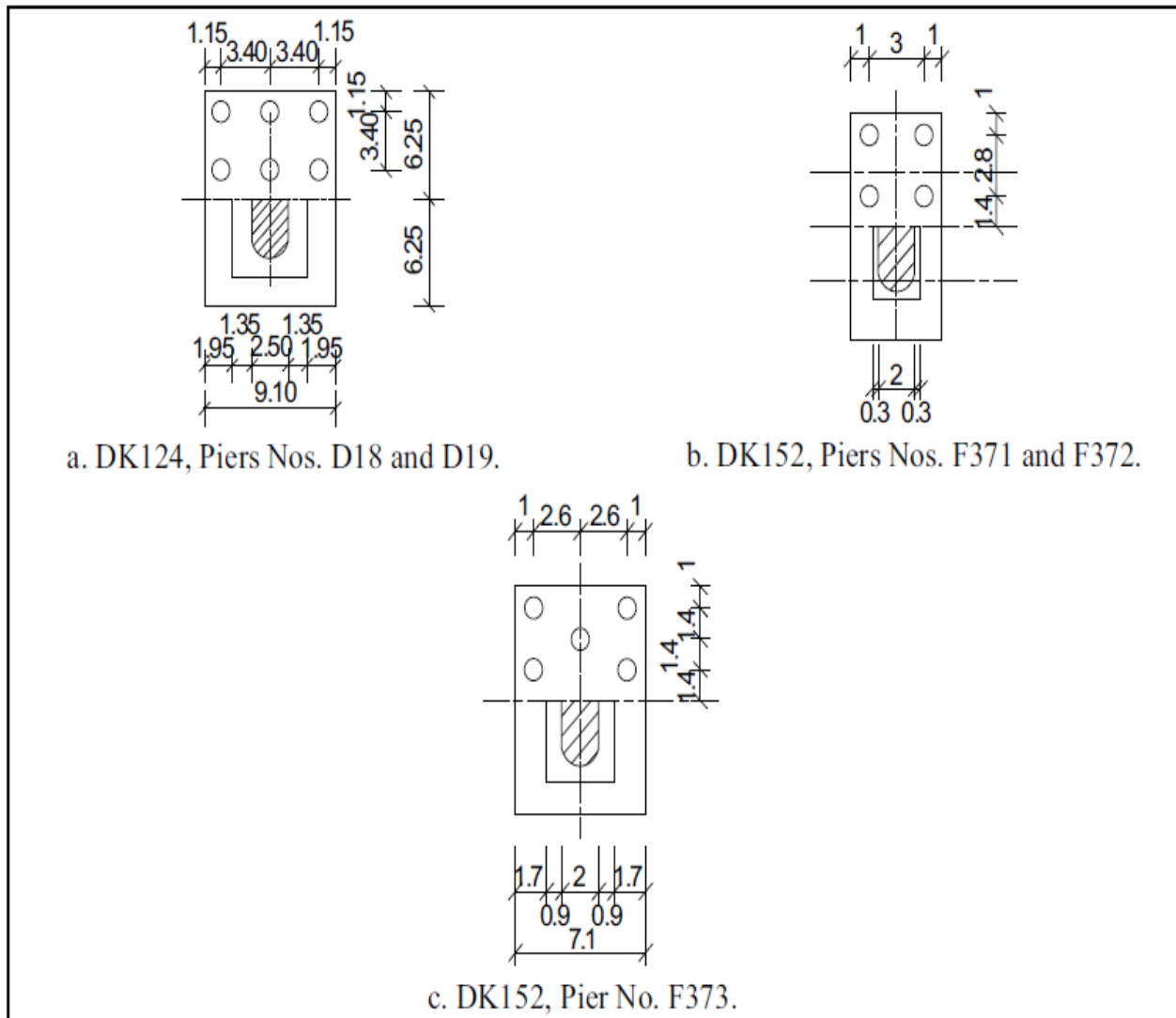


Fig. (6). Sketches of the Beijing-Shanghai high-speed railway bridge piers at locations DK124 and DK152 (all the dimensions in meter).

the piles is 3.4 m in both directions, length of piles is 52 m. The bridge at DK152 worksite as shown in Figs. (6.B and 6.C) is supported by reinforced concrete pile groups, which consist of 8 bored piles for F371 and F372 piers and 10 bored piles for F373 pier with a pile diameter of 1.0 m for F371, F372 and F373. The pile length is 50 m for F371 and F372, and 47 m for F373. The caps are rectangular with a length of 10.4 m and a width of 5 m for F371 and F372 piers, and a length of 10.4 m and a width of 7.1 m for F373 pier. The caps thickness is 0.55 m for the upper cap and 2.2 m for the lower cap for F371 and F372, while for F373 is 1.1 m for the upper cap and 2.2 m for the lower cap. The groundwater levels below the ground surface are 1.4 m for D18, 2.3 m for D19, 1.6 m for F371 and 1.2 m for both of F372 and F373. Figs. (7 and 8) are showing the classification sketches of the soil layers of the Beijing-Shanghai high-speed railway bridges at locations DK124 and DK152 respectively. The site investigations show that there is a need of a number of soil layers for the deep soft soils because when the base bottom layer is not stable anchorage in the soft soil or rock layer

is difficult to monitor. The span length of the bridge at both worksites is 32m.

2.3. Data Used in the Study

The data used in this study were taken from gauge level measurements of pile foundations processed for Beijing-Shanghai project at locations DK124 and DK152 that started on 2009-10-27. The measurements collected using the single point of account settlement meter to estimate the thickness of the deep soft soils included the displacement/mm and the relative amount of compression/mm. These values were measured for multiple depths and at different time intervals. The reading depths were different depending on the depth of the compressed layer under the pile. The study represented these data in a graphical form of the experimental results to predict settlement of deep soft soils. Tables 1 and 2 show the geotechnical properties and parameters of the soft soil in the DK124 and DK152 worksites, respectively.

Table 1. Soil Characteristics and Strength Parameters at the DK124 Working Points

Sampling depth (m)	ω %	γ_{unsat} (kN/m ³)	γ_{sat} (kN/m ³)	e	k (m/day)	ν	a_v (MPa ⁻¹)	c (kPa)	ϕ (degree)	ψ (degree)
1.07	30.7	17.7	18.0	0.849	0.086	0.32	0.51	14	8.5	0.0
4.37	27.4	18.3	18.6	0.813	0.086	0.31	0.17	15.9	9.2	0.0
9.37	31.1	18.2	18.5	0.852	0.432	0.32	0.47	11.0	10.6	0.0
19.57	26.7	19.4	19.5	0.756	0.432	0.30	0.41	25.6	13.5	0.0
24.82	22.9	19.3	19.5	0.651	0.432	0.30	0.25	20.9	16.7	0.0
26.37	24.2	20.4	20.6	0.658	0.864	0.29	0.32	21.4	30.8	0.8
30.72	26.0	18.7	18.9	0.737	0.086	0.29	0.23	96.8	14.6	0.0
41.97	28.2	18.9	19.2	0.804	0.432	0.28	0.31	35.6	15.5	0.0
46.27	24.7	19.2	19.4	0.677	0.432	0.28	0.13	42.0	21.3	0.0
53.07	30.6	19.4	19.7	0.887	0.043	0.27	0.20	43.8	17.1	0.0
57.57	27.4	20.0	20.2	0.772	8.64	0.28	0.29	8.9	32.7	2.7
69.57	18.9	19.4	19.7	0.587	0.043	0.27	0.18	43.8	17.1	0.0
73.17	28.2	20	20.2	0.820	8.64	0.28	0.34	8.9	32.7	2.7
80.67	23.9	19.2	19.5	0.685	0.043	0.27	0.23	44.7	15.5	0.0
83.57	23.2	20.2	20.4	0.673	8.64	0.28	0.24	13.7	36.2	6.2

Where: ω : Water content; γ_{unsat} : The unsaturated unit weight of soil; γ_{sat} : The saturated unit weight of soil; e : Void ratio; k : Permeability; ν : Poisson's ratio; a_v : Compression Index; E_s : Compression modulus; c : Cohesion; ϕ : Internal friction angle; ψ : Dilatancy angle.

Table 2. Soil Characteristics and Strength Parameters at the DK152 Working Points

Sampling depth (m)	ω %	γ_{unsat} (kN/m ³)	γ_{sat} (kN/m ³)	e	k (m/day)	ν	a_v (MPa ⁻¹)	c (kPa)	ϕ (degree)	ψ (degree)
3.3	30.7	17.7	18.9	0.849	0.086	0.30	0.51	52.5	14.8	0.0
13.7	27.4	18.6	18.9	0.813	0.432	0.30	0.17	16.6	11.2	0.0
16.2	31.1	19.4	19.6	0.852	0.432	0.30	0.47	17.0	13.2	0.0
21.4	26.7	19.7	20.0	0.756	8.64	0.28	0.41	6.8	37.7	7.7
25.5	22.9	19.4	19.6	0.651	0.432	0.30	0.25	17.0	13.2	0.0
28.1	24.2	19.9	20.6	0.658	0.864	0.29	0.32	14.8	29.1	0.0
30.3	26.0	19.1	19.3	0.737	0.432	0.28	0.23	35.8	20.1	0.0
34.2	28.2	18.9	19.2	0.804	0.864	0.29	0.31	31.4	24.5	0.0
38.7	24.7	19.8	20.0	0.677	8.640	0.28	0.13	6.8	37.7	7.7
41.7	30.6	18.3	18.4	0.887	0.086	0.31	0.20	30.0	11.2	0.0
43.4	27.4	19.3	20.2	0.772	0.086	0.29	0.29	18.0	11.5	0.0
51.3	18.9	19.5	19.6	0.587	0.043	0.27	0.18	29.0	18.0	0.0
55.1	28.2	19.0	20.2	0.820	0.086	0.29	0.34	38.5	10.9	0.0
64.7	23.9	19.2	19.4	0.685	0.086	0.29	0.23	42.3	21.8	0.0
73.0	23.2	19.9	20.4	0.673	8.64	0.28	0.24	11.6	39.0	9.0

2.4. Construction Loading

The dead load of the bridge, pile foundation dimensions and compression soil stratum for both DK124 and DK152

worksites are shown in Tables 3 and 4. Therefore, the relationship between the construction loads and settlement readings with the construction progression can be observed.

Table 3. Locations of Point pier Foundation Test Sections

Worksite	Pier No.	Number of Piles	Pile length (m)	Pile Diameter (m)	Pile Cap Length×Width (m×m)	Load (tons)	Compression Stratum (kPa)
DK124	D18	12	52	1.25	13×9.1	2100	Silt 200
	D19	12	52	1.25	13×9.1	2100	Silt 200
DK152	F371	8.0	50	1.00	10.4×5.0	1472	Silty clay 250
	F372	8.0	50	1.00	10.4×5.0	1487	Silty clay 250
	F373	10	47	1.00	10.4×7.1	1502	Silty clay 250

Table 4. Construction Loads at Each Location

Worksite	Bridge Name	Pier No.	Pier loads (tons)	Beam Load (tons)	Secondary Dead Load (tons)	Total (tons)
DK124	Tianjin Bridge	D18	481.25	1202.76	425.6	2109.61
DK152		F373	240	836.8	425.6	1502.4

2.5. Settlement Analysis

Tables 5 and 6 summarize the results of the compression readings in the field within the compressed soil layers. The standard of adjacent measurement based points on each meter of soil compression is between 0.1 mm and less. Therefore, from Tables 5 and 6, it can be estimated that the thickness of the compressed layer is equal to 9.5 m and 10 m for DK124 and DK152 worksites, respectively. The monitoring was done by using the single point of account settlement meter to estimate the compressed layer thickness which is considered as a difficult task in the deep soft soil area.

The monitoring points were located at the mid-point on the upper and lower pile caps, respectively. The settlement readings during the bridge construction were measured at the pile tip with different levels of gauges, as shown in Fig. (9) for pier No. 18 at worksite DK124. The negative sign indicates the direction of the settlement. The readings showed that the settlement increased but after sometimes decreased with the passage of time after the completion of girder con-

struction. This may be attributed to the fact that the foundations were backfilled during the monitoring of points on the piers. Unfortunately, at various times during construction, the survey reference points were either obstructed or filled over before reference elevations could be obtained by surveying multiple points [10].

Figs. (9 and 10) show the relationship between settlement and the reading dates for different depths during the construction loads of piers No. 18 and 19 at worksite DK124. Fig. (11) shows the same relationships for piers F371, F372 and F373 at worksite DK152. The results of the field tests at worksite DK124 show a maximum settlement of 7.0mm at pier D18 and 7.1 mm at pier D19, while at worksite DK152, the maximum settlements at piers F371, F372 and F373 are 9.0 mm, 8.7 mm and 8.1 mm, respectively.

From Figs. (10 and 11), it can be observed that the settlement-load-time curve can be divided into three segments. When the load is less than 5 MN, the settlement of the pile cap increases to amount of about 4 mm for piers at DK124

Table 5. DK124 Worksite Compression Results for Compressed Layer (piers D18 and D19)

Location (m) (under the pile tip)	Compression (mm)			Average compression (mm)	Compression per meter between adjacent measurement points (mm)
	2010-10-24	2010-11-21	2010-12-6		
0.5	2.72	2.72	2.71	2.72	5.43
2.3	3.12	3.14	3.13	3.13	0.23
4.5	4.28	4.28	4.28	4.28	0.52
4.6	4.41	4.42	4.42	4.42	1.37
9.5	4.86	4.86	4.87	4.86	0.09
13.6	5.15	5.16	5.18	5.16	0.07
18.5	5.10	5.11	5.12	5.11	~0.0
27.5	5.56	5.58	5.58	5.57	0.05

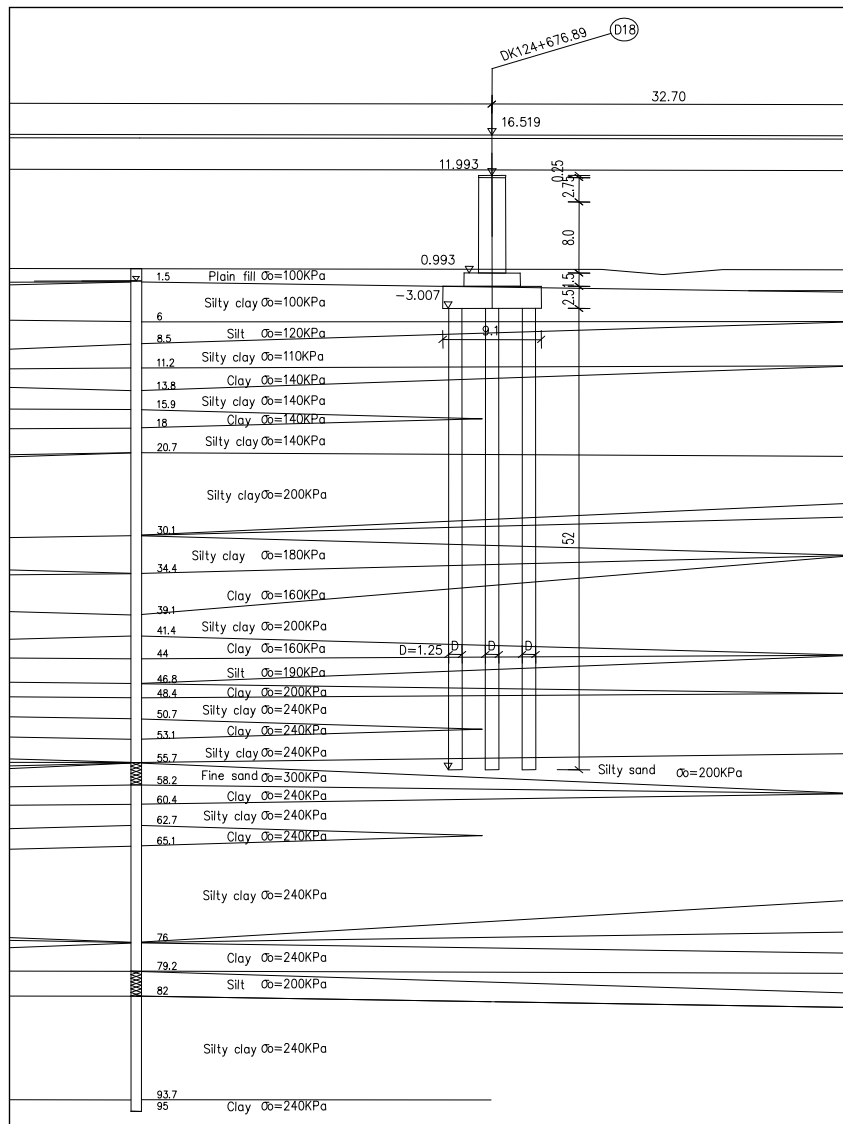


Fig. (7). Sketch of the soil layers of Beijing-Shanghai high-speed railway bridge at location DK124, D18 (all the length dimensions in meter).

Table 6. DK152 Worksite Compression Results for Compressed Layer (piers F371 and F372)

Location (m) (under the pile tip)	Compression (mm)			Average compression (mm)	Compression per meter between adjacent measurement points (mm)
	2010-10-24	2010-11-21	2010-12-6		
0.5	4.12	4.13	4.13	4.13	8.25
5	5.94	5.95	5.93	5.94	0.40
10	6.38	6.39	6.39	6.39	0.09
20.3	6.49	6.51	6.51	6.50	0.01
25.35	6.55	6.56	6.58	6.56	0.01

and 7 mm for piers at DK152. When the load increases from 5 MN to 17 MN at DK124 and from 5 MN to 10 MN at DK152, the settlement of the pile cap reaches 6.5 mm and 8 mm respectively, which is an increase of 100%. When the load increases from 17 MN to 20 MN for DK124 and from 10 MN to 15 MN for DK152, the increase in the settlement

of the pile cap is small; the settlement becomes stabilized and the total settlement is approximately 7 mm for the piers at DK124 and 9 mm for the piers at DK152.

The above results show that the maximum settlement values measured in the field are within the limits allowed by the standard specifications. The TB10002.5-2005 code

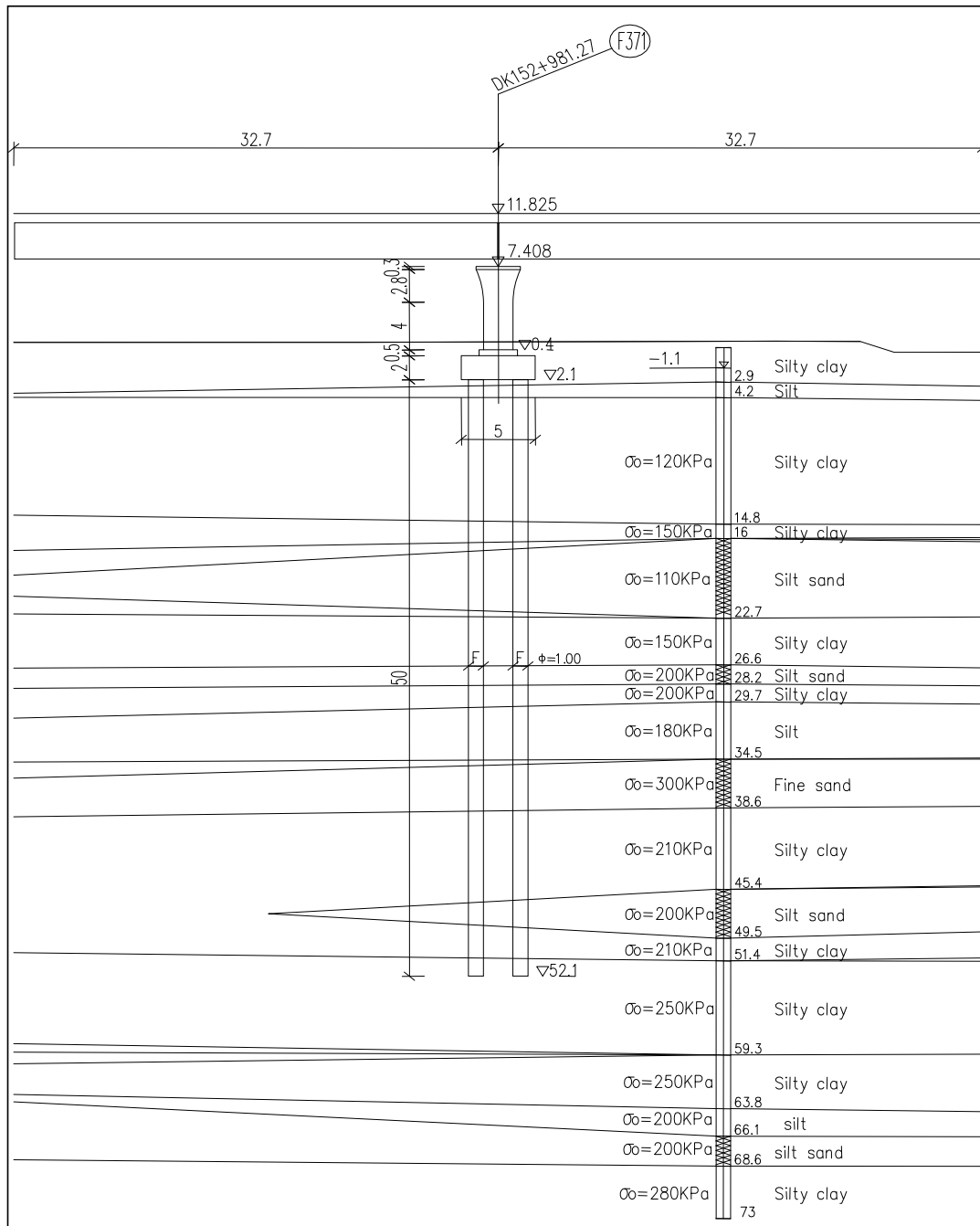


Fig. (8). Sketch of the soil layers of Beijing-Shanghai high-speed railway bridge at location DK152, F371 (all the length dimensions in meter).

(3.2.1) specifies an allowable settlement of 40–80 mm [11], and the code for “200 kilometre per hour passenger railway interim design provisions” specifies an allowable settlement of 50 mm [12]. Ballast railways have two requirements: the allowable settlement of a single foundation must be not more than 80 mm, while two adjacent foundations may have settlement of not more than 40 mm. The foundations for simply supported deck bridges are frequently designed for differential settlement with relative rotations of up to 1/800 (40 mm in a 32 m span) [13]. In reasonably homogeneous soils, differential settlements between adjacent foundations are often

assumed to make up half of the total settlement. Thus, under these criteria the total measured settlement of the bridge is less than the allowable settlement.

2.6. Problem Statement

Foundation design like other structural design requires a good sound basic approach in order to achieve a truly successful result [14]. The stability of the structure depends upon the stability of the supporting soil, the foundation must not settle beyond a tolerable limit to avoid damage of the

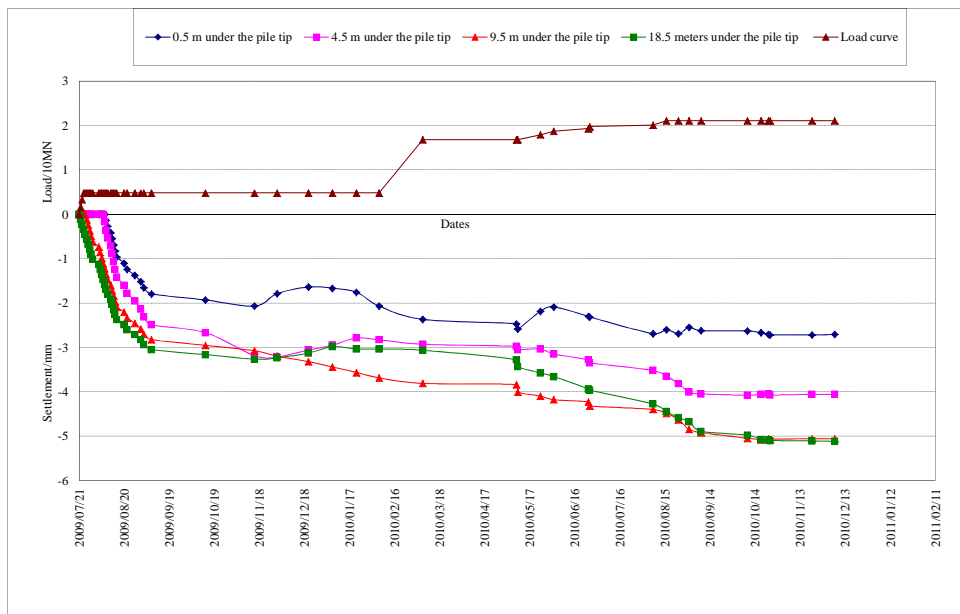


Fig. (9). Compression settlement of pier D18 at DK124.

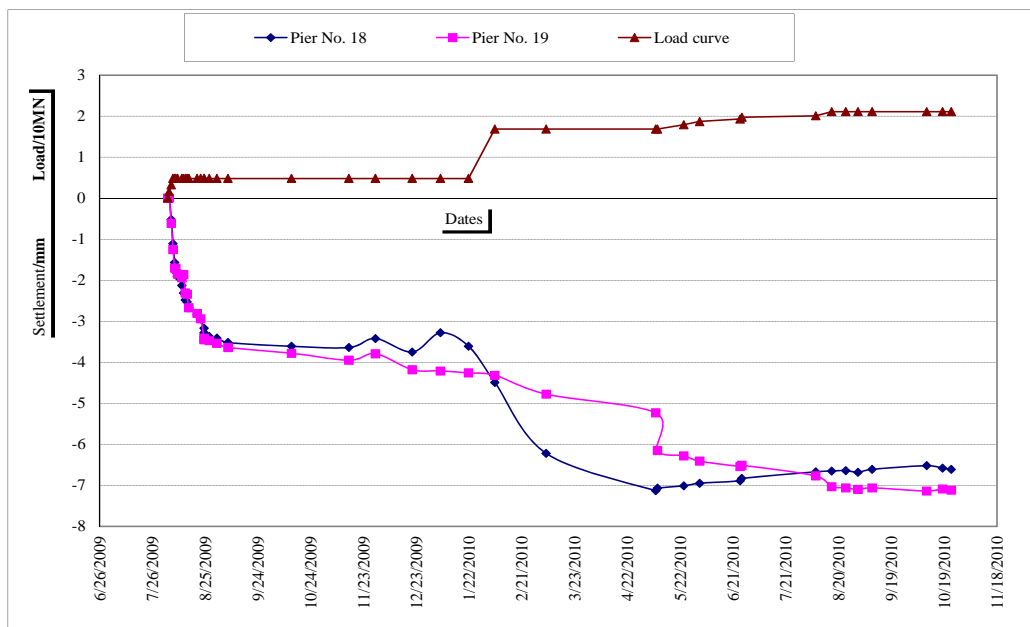


Fig. (10). Compression settlement of piers D18 and D19 at DK124.

structure [15]. Structures built on deep soft soils are prone to excessive settlement. A large portion of this settlement is attributed to the consolidation process, which may continue for an extended period depending on the soil’s ability to dissipate the excess pore water pressure imposed by the construction loads. The relationship between settlement and time is not linear because a large percentage of settlement usually takes place early in the timeline [16]. The consolidation characteristics of the soil are influenced by numerous factors including the size and shape of the soil particles, the moisture content, permeability, initial density and physical and chemical properties of the soil. Predicting the amount of settlement is possible after the soil characteristics have been determined, and the determination of pressure distribution below the loaded area which is due to the estimated structural loading [17]. It is mentioned previously that the deter-

mination of the compressed layer thickness is considered as a difficult task in the deep soft soil area. This problem has been solved for this project using the single point of account settlement meter in the field. The other difficulty is to find the suitable way to predict the long-term of settlement to show its effect on the structure. The next sections show the developed results of the settlement obtained from the numerical analysis.

3. RESULTS AND DISCUSSIONS

3.1. Settlement Prediction by Hyperbolic Modeling

Settlement prediction through the use of a hyperbolic function assumes an average settlement speed that is used to predict the long-term settlement based on initially measured settlement amounts. The hyperbolic method has been shown

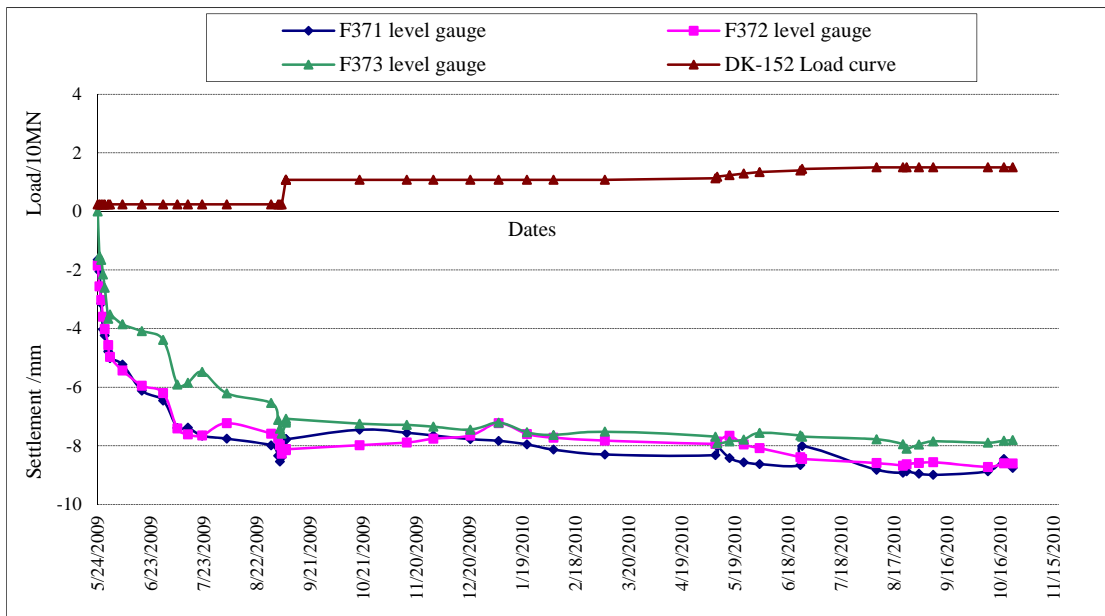


Fig. (11). Compression settlement of piers F371, F372 and F373 at DK152.

to be useful for settlement prediction in complex soil formations. It is demonstrated that the hyperbolic method is applicable to infinitesimal strain, finite strain, nonlinear soil properties, and non homogeneous soil conditions [18]. The hyperbolic method can be used for settlement estimation of highly compressible soils [19]. However, when an appreciable portion of the settlement is due to secondary compression, settlement prediction based on the slope of the initial linear portion of the hyperbolic plot requires a correction factor that would depend on the amounts of secondary compression. Although the inverse of the slope of the hyperbolic curve's final linear portion can provide reasonable estimates of the total settlement including secondary compression, establishing the curve slope requires data beyond 90% consolidation, and this renders the hyperbolic method less useful for practical applications [20]. The settlement can be calculated at any time after loading completion through the use of the following equation [21].

$$S = S_0 + (t / (\alpha + \beta \times t)) \tag{1}$$

Where: S is the settlement amount at time t in mm, S_0 is the initial settlement amount (at the time of completion of girder construction according to the field measurements) in mm, t is the time in days. α and β are the coefficients, after a straight line is calculated, the coefficients α and β can be calculated for the intersection of the line with the vertical axis and slope of the line, respectively, as shown in Fig. (12). Values of $\alpha = 8.394$ and $\beta = 0.505$ are found to be according to the data for pier No. 18, and pier No. 19 has the values of $\alpha = 30$ and $\beta = 0.25$. The predicted settlement values for piers Nos. 18 and 19 are obtained through using equation 1 as shown in Figs. (13 and 14), respectively.

Figs. (13 and 14) clearly show the settlement field measurements of the loads imposed, with the required construction time, in addition to the predicted settlement for a period longer than that of the field test. The results show that long-term settlement will not be large as compared to the site measurements. The predicted settlement values are about 6.5

mm for pier No. 18, and 8 mm for pier No. 19 in the DK124 worksite. The predicted curves closely match the experimental curves and indicate that the structure will not be affected by the long-term consolidation. The initial settlement was considered for this model at the time of beam girder construction. After this initial value, the settlement increased abruptly to reach its maximum predicted value.

As shown in Figs. (15 and 16), the long-term settlement predicted by the hyperbolic model for piers F371 and F373, respectively closely matched the field test results. The piers F371 and F373 have coefficient values of $\alpha = 80$, $\beta = 0.761$ and $\alpha = 45$, $\beta = 1.29$, respectively.

3.2. Settlement Prediction by Statistical Regression

Regression analysis is one of the most commonly used analysis of the statistical tools. The estimated regression equation is a function of the estimates of the slope and intercept [22,23]. Different constants may be added to variables to yield the original variables which are to be used in the

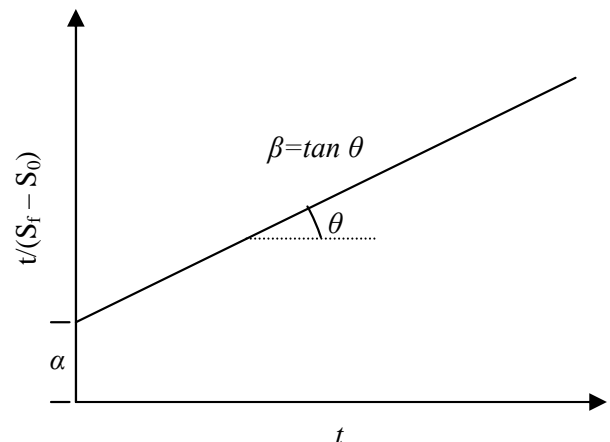


Fig. (12). Hyperbolic function curve coefficient calculation.

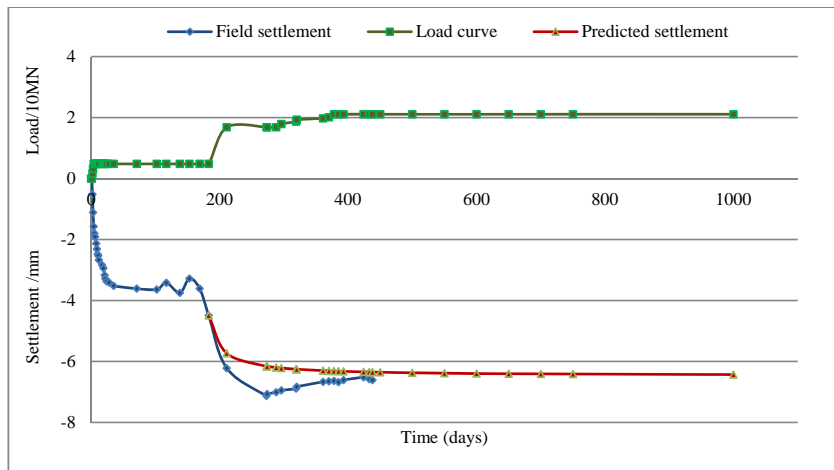


Fig. (13). Field settlement, load overtime and predicted settlement curves for pier No. 18.

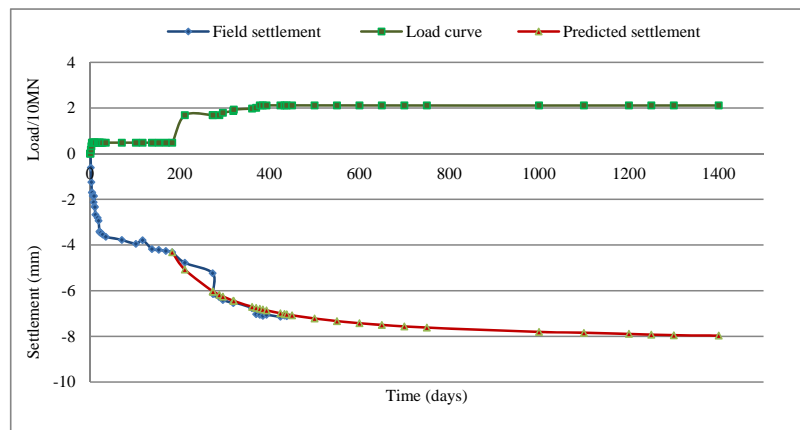


Fig. (14). Field settlement, load overtime and predicted settlement curves for pier No. 19.

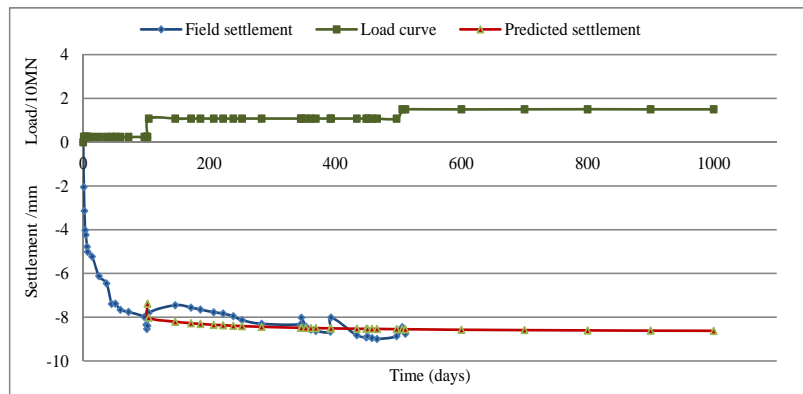


Fig. (15). Field settlement, load overtime and predicted settlement curves for pier No. F371.

simple linear regression model [24]. In this study, the SAS software is used to obtain the settlement prediction by considering the time and load as independent variables and the settlement reading as dependent variable [25]. Appendix A shows the log file of the input program that is used to find the output results. From the analysis, the following equation is derived for pier 18:

$$S_{118} = -0.812 - 2.674 L - 0.015 t + 0.007 Lt \tag{2}$$

Where: S_{118} is the settlement value for pier 18 at time t in mm, L is the load/10 MN and t is the time in days.

The first parameter of the above equation constituted the initial value of settlement and this parameter represented the intercept variable in the statistical analysis. The settlement during the testing time and settlement prediction can be calculated by equation 2 for pier 18 as shown in Fig. (17).

For pier F372 at worksite DK152, the statistical equation is derived from the field data as shown in the following:

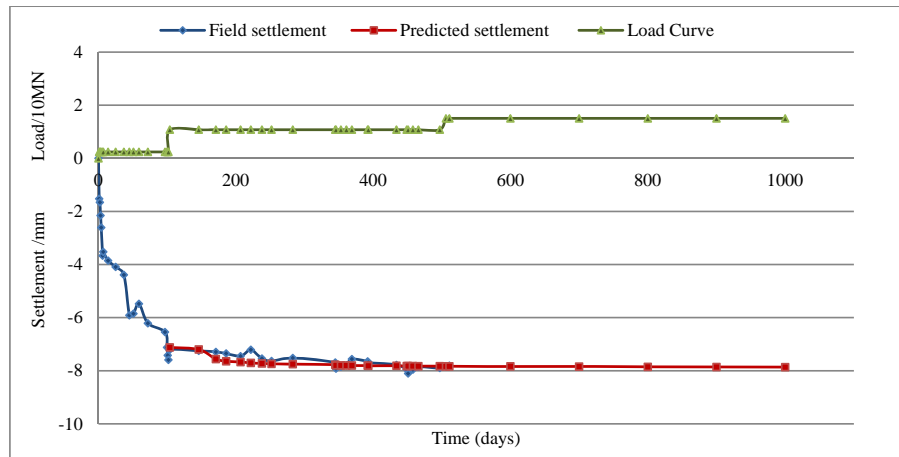


Fig. (16). Field settlement, load overtime and predicted settlement curves for pier No. F373.

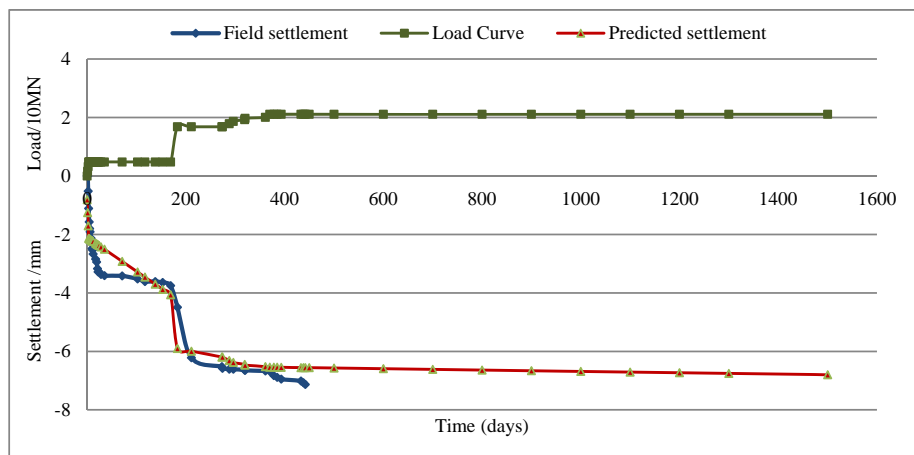


Fig. (17). Settlement at pier No. 18 calculated by the statistical regression method.

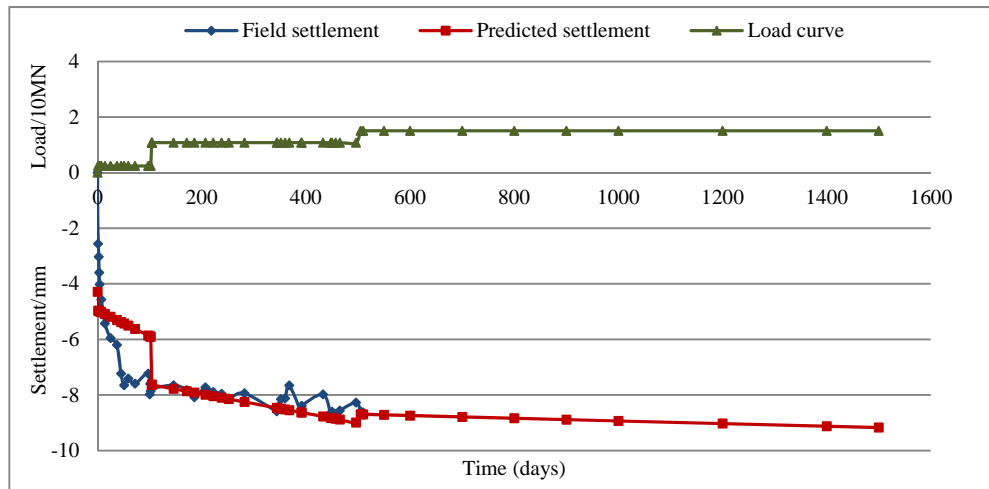


Fig. (18). Settlement at pier No. F372 calculated by the statistical regression method.

$$S_{iF372} = -4.291 - 2.771 L - 0.011 t + 0.007 Lt \quad (3)$$

Based on the results obtained by applying equation 3 of the statistical analysis, as shown in Fig. (18), the statistical regression method is appropriate to predict the settlement for long period. The predicted settlement has a slight downward trend but remains controlled and within the limits allowed for the long-term settlement. In the statistical analysis, the

data have random readings; therefore, they are adjusted for this aspect to get better results and this may be considered as disadvantage in the statistical regression.

From the results obtained in the output of the program shown in Appendix A, the pattern in Fig. (19) indicates that it may assume that the residuals are not normally distributed and constant in variance at each level of the predicted values.

Also, according to QQ-plot analysis, the data are supposed to be normally distributed if the plot forms a straight line, whereas if the plot creates some upward or downward curvatures, the data are supposed to be right-skewness and left-skewness, respectively. In the QQ plot shown in Fig. (20), the up and down wave form supports indicated that the predicted settlement is not normally distributed. Therefore, the previous discussion explains that the data of the project used in this study are difficult to be analyzed by the statistical models, so the next sections will deal with the three dimensional finite element analysis with new modification to get better results of settlement in the deep soft soils.

3.3. Finite Element Numerical Analysis with Plaxis 3D

Three-dimensional finite element numerical analysis in Plaxis program is used to verify the models shown in Figs. (6, 7 and 8) to calculate the settlement parameters. The program took the soil’s characteristics and strength parameters into consideration. In the finite element analysis, a Mohr-Coulomb model with drained conditions is used to simulate the soil material, the soil around the pile is expected to be subjected to large deformations; therefore a non-linear material model is used. The pile-soil interface is modeled by the

interface element with Mohr-Coulomb. A linear elastic non-porous material model is used to represent the piles and pile cap of the reinforced concrete structure. The bored piles shaft shape is circular with different diameters and depths for each pier as mentioned previously. A 3D model is used for modeling a vertical pile in a clay deposit by including the elastoplastic behavior of soil and slippage of soil due to axial load [26,27].

The model required five basic input parameters: Compression modulus, E_s ; Poisson’s ratio, ν ; cohesion, c ; friction angle, ϕ ; and dilatancy angle, ψ . The implications of these requirements are appreciated by considering the Mohr-Coulomb equation in the following form [28]:

$$S_{u0} = c'_m + (\sigma - u) \tan\phi'_m \tag{4}$$

Where, S_{u0} is the shear strength. The parameters c'_m and ϕ'_m are the cohesion intercept and friction angle mobilised at yield, σ is the applied normal stress and the pore water pressure, u , is the sum of hydrostatic or steady-seepage pore water pressure u_0 and the shearing pore water pressure Δu . The finite element mesh models of DK124 and DK152 are shown in Figs. (21 and 22), respectively.

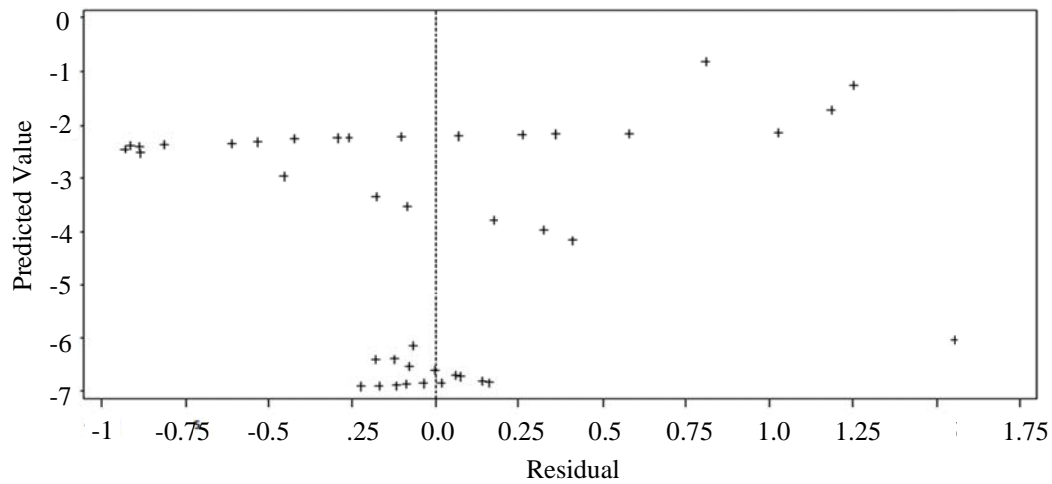


Fig. (19). Residual versus predicted value at pier No.18.

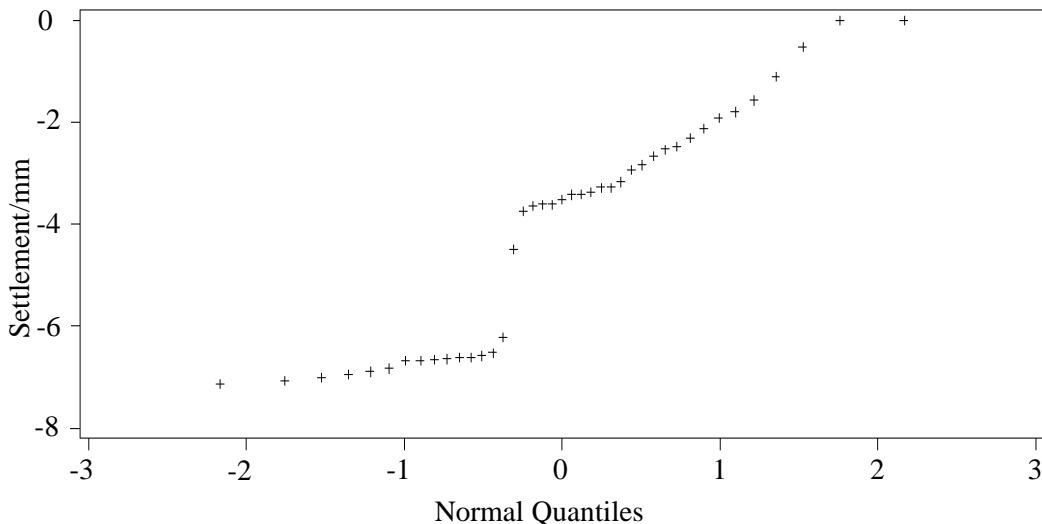


Fig. (20). Settlement versus normal quantiles at pier No.18.

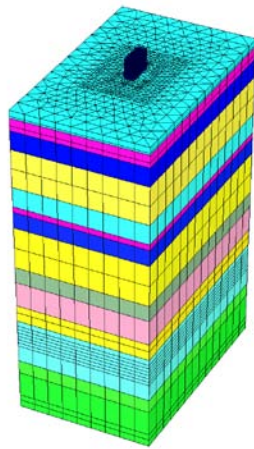


Fig. (21). FEM mesh model of DK124.

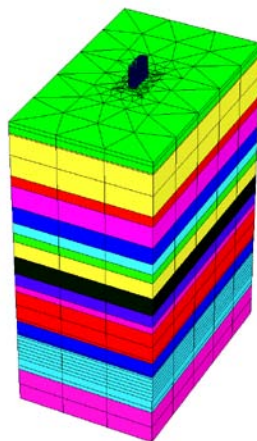


Fig. (22). FEM mesh model of DK152.

3.3.1. New Formula for Compression Modulus Estimation

The most difficult part of a settlement analysis is the evaluation of the compression modulus E_s that would conform to the soil condition in the field [29]. As already noted above, in connection with the characteristics of finite element method, we put forward a formula of compression modulus related to soil layer depth in natural state:

$$E_{s,z} = E_{s,0.1-0.2} \cdot (z/h_0)^{1/\beta} \tag{5}$$

In the Eq. (5): β is the parameter, the value is taken from Table 7; z is the depth of soil layer, m; h_0 is a reference depth, it can be used as $h_0=1\text{m}$; $E_{s,0.1-0.2}$ is the compression modulus under the pressure of 0.1~0.2MPa, this value can be used from soil test report, MPa.

This is a formula of compression modulus related to soil layer depth. In the process of calculation by finite element method, on the basis of the value of soil test report, the variation value of compression modulus along with the soil depth is obtained by the proposed equation.

Eq. (5) can provide conservative calculated values for compression modulus by which the results of Plaxis 3D Foundation program will be more accurate and approaching to the real behavior of settlement in the field. Using above equation will increase the value of compression modulus $E_{s,0.1-0.2}$, therefore, the increase of the soil compression modulus will reduce the overall settlement [30,31]. In Appendix B, Figs. from B.1 to B.7 show the field values of $E_{s,0.1-0.2}$ for both DK124 and DK152 worksites as compared to the maximum and minimum values of modified calculated compression modulus. The consistency of the soils is according to the specifications of the British standard code (BS) [32]. In the BS code, fine soils are divided into *ten* classes based on their measured plasticity index and liquid limit values: clays are distinguished from silts, and five divisions of plasticity are defined (see Table 8 and Fig. 23):

According to the specifications of the soil plasticity maintained using Table 8 and Fig. (23); the value of β can be found in Table 7 and Eq. (5) can be applied to calculate the modified compression modulus. Table 7 shows the value of β for more cohesive and less cohesive soils, also it can be used to modify the theoretical calculations of the soil settlement which depend on the compression modulus as a parameter for this aspect.

The compression modulus of clayey soils is usually assigned with very high correction factors. It is demonstrated that the basic reason to correct these modulus is the requirement to account for the effect exerted by so-called leakage pressures on the skeleton of the soil specimens being tested. These leakage pressures are developed due to the fact that

Table 7. Value of β

Value of β^*	Name and characteristics of soil layer
2.5~3.5	Cohesive soil, silt: solid, hard plastic; Sandy soil: medium-density and above that; Sandy gravel soil: with good grading.
3.5~5	Cohesive soil, silt: plastic; Sandy soil: a little more density than common sandy soil to medium-density; Sandy gravel soil: with not good grading.
5~8	Cohesive soil, silt: plastic to soft plastic; Sandy soil: loose to a little more density than common sandy soil.
8~10	Cohesive soil, silt: soft plastic to worse.

*: The increasing stiffness is the smaller value of β .

Table 8. Plasticity of the Soil According to the Liquid Limit Values (BS Code)

Low plasticity	$w_L = < 35\%$
Intermediate plasticity	$w_L = 35 - 50\%$
High plasticity	$w_L = 50 - 70\%$
Very high plasticity	$w_L = 70 - 90\%$
Extremely high plasticity	$w_L = > 90\%$

Where: w_L is the liquid limit of soil.

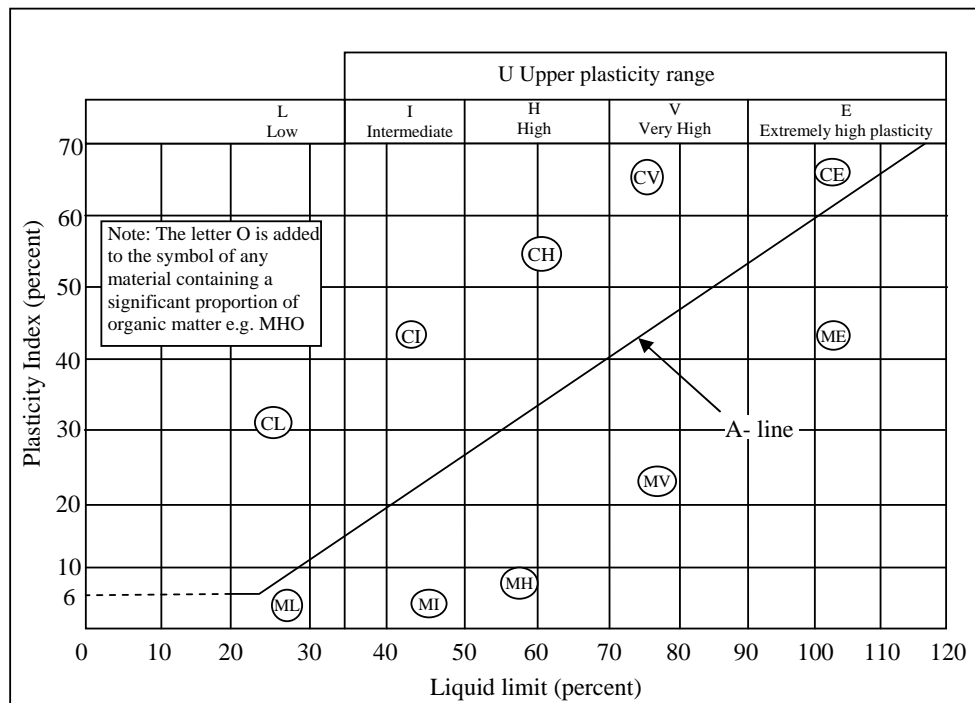


Fig. (23). Plasticity chart for the classification of fine soils and the finer part of coarse soils (measurements made on material passing a 425 mm sieve, in accordance with BS 410).

consolidation filtration in soils is only possible when certain initial pressure gradients are attained [33].

3.3.2. Construction Sequence and Calculation Items

A finite element analysis of any physical problem requires that a mesh of finite elements should be generated. The generation of finite element meshes is a fundamental step and may require significant human and computational efforts [34]. The loads due to construction above the pile cap are transmitted to the top surface of the pile cap through the bridge pier. These loads can be as considered uniformly distributed loads. The pressure applied in the model is calculated by dividing the total construction load by the area of the pier. The pier area is about 15.9 m² for DK124 and 11.15 m² for DK152, which represents the pressure area on the top of the pile cap and pressure can be calculated corresponding to the different construction stages. A total of twelve calculation steps are performed, as follows.

Step 0: The gravity is applied to the original configuration, simulating the initial field stress.

Step 1: Construction is started from drilling holes until completion of the pile construction. During construction, consolidation occurs in soils and settlement of the pile group is achieved.

Step 2: Construct the lower pile cap to the designed thickness; the construction of the lower pile cap is completed.

Step 3: The same as above in step 2 but for the upper pile cap.

Steps 4-12: A greater load is applied. This load is equivalent to the construction loads sequence for each bridge.

The material properties of the piles and pile cap which is used in the models are shown in Table 9.

The above steps are applied in the Plaxis program by taking into consideration the modified values of compression modulus calculated by Eq. (5). The results of the numerical analysis for piers D18 and D19 in DK124 worksite are shown in Figs. (24 to 27). The final vertical displacement value in Fig. (24) is about -13.71 mm; the minus sign refers

Table 9. Material Parameters for Pile Foundation

Worksite	Item	Unit Weight (kN/m ³)	Poisson Ratio	Compression Modulus (GPa)
DK124, DK152	Pile Cap and Pile	25	0.15	30

to the direction of the displacement. This value is close as compared to the maximum values shown in Fig. (10) and gives good indication when considering the numerical analysis. The values of incremental displacement, total Cartesian strain and active pore water pressure are adequate as shown in Figs. (25, 26 and 27), respectively. Fig. (27) shows the active stress scenario in the soil; the pore pressure gives in-

dication that it would not increase the final value of the consolidation settlement by the effect of train loads and secondary compression.

In the same manner Figs. from (28 to 31) represent the results of the numerical analysis for DK152, piers F371 and F372. The total vertical displacement is -13.5 mm as shown in Fig. (28); this value is also close from the field measurements (see Fig. 11) and gives appropriate indication for the 3D numerical to calculate the settlement in the deep soft soil area. The other numerical calculations represented by the incremental displacement, total Cartesian strain and active pore water pressure are shown in Figs. (29, 30 and 31), respectively. The above numerical calculations indicate the

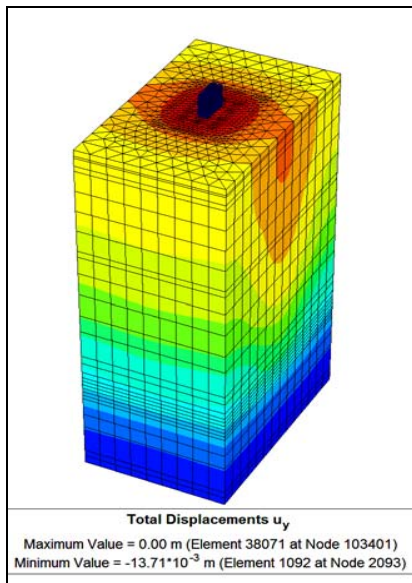


Fig. (24). Total vertical displacement (U_y) for soil layers of the DK124 model.

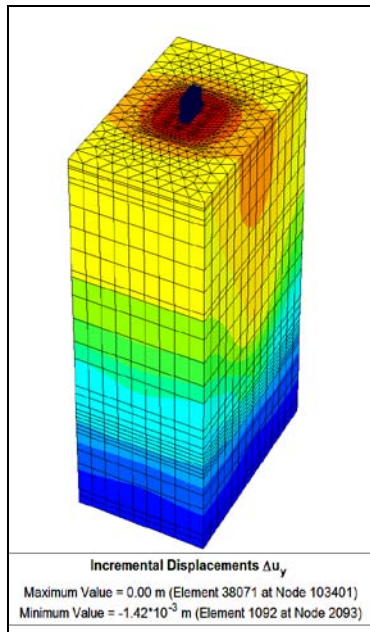


Fig. (25). Incremental displacement for soil layers of the DK124 model.

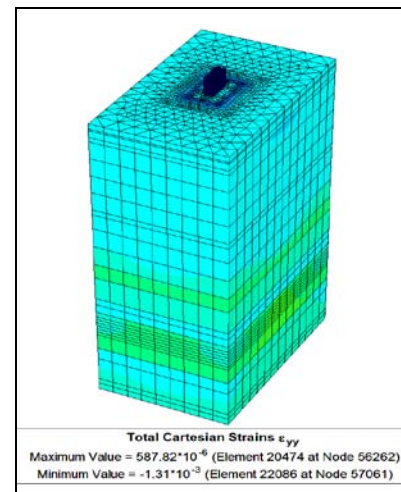


Fig. (26). Cartesian total strain for soil layers of the DK124 model.

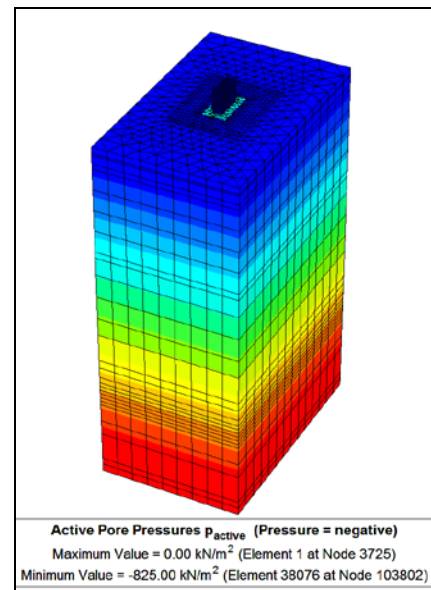


Fig. (27). Active pore pressure for soil layers of the DK124 model.

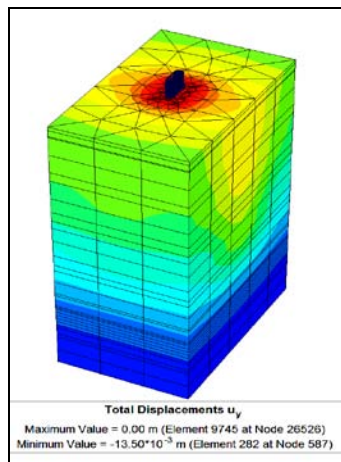


Fig. (28). Total vertical displacement (U_y) for soil layers of the DK152 model.

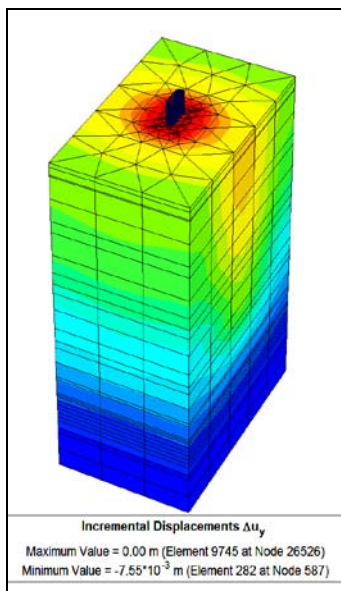


Fig. (29). Incremental displacement for soil layers of the DK152 model.

normal operations of the soil and the design satisfy of the project. The numerical analysis of finite element may provide a precious way to predict the settlement by considering the new modification in calculating the compression modulus and applying the correct procedure for simulating the data in the program. Figs. (32 and 33) show the calculated results for the simulation of the pile installation sequence as compared to the measured results obtained from the field monitoring through which it can be observed that appropriate results obtained using the empirical equation.

In Appendix C, Figs. from (C.1 to C.8) show the results of the numerical analysis for both models DK124 and DK152, without using the new empirical equation to calculate the compression modulus E_s that is used in the Plaxis program. The results of the total vertical displacements are -29.36 mm for DK124 and -39.67 mm for DK152 as shown in Figs. (C.1 and C.5), respectively. These values are far from that measured in the field which give a good indication and confidence to the results obtained using the proposed

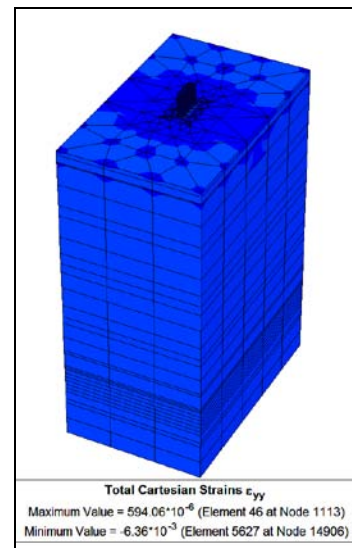


Fig. (30). Cartesian total strain for soil layers of the DK152 model.

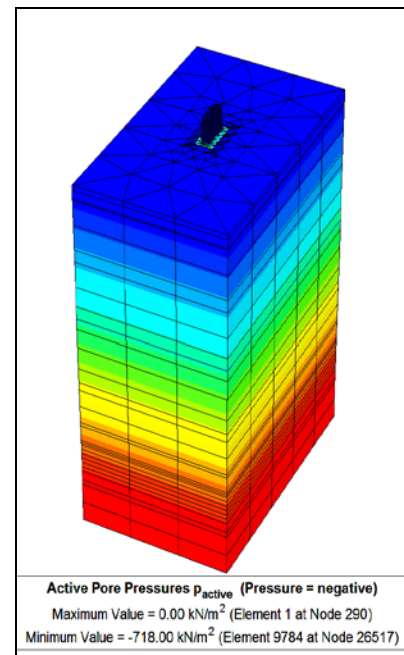


Fig. (31). Active pore pressure for soil layers of the DK152 model.

equation of compression modulus. Besides the other parameters calculated and represented by the incremental displacement, total Cartesian strain and active pore water pressure as shown in Figs.(C.2, C.3 and C.4) for DK124 and C.6, C.7 and C.8 for DK152, are also far different from the real behavior of the soil. Therefore, the new formula used in this paper can modify the results of the numerical analysis calculated by the three dimensional Plaxis program and can be applied in the norms calculations, which depend on the compression modulus to estimate the settlement.

CONCLUSION

The field tests of Beijing-Shanghai bridges show the settlement values and explain the process of consolidation over construction time. The field measurements show new technique to estimate the thickness of compressed layer which is

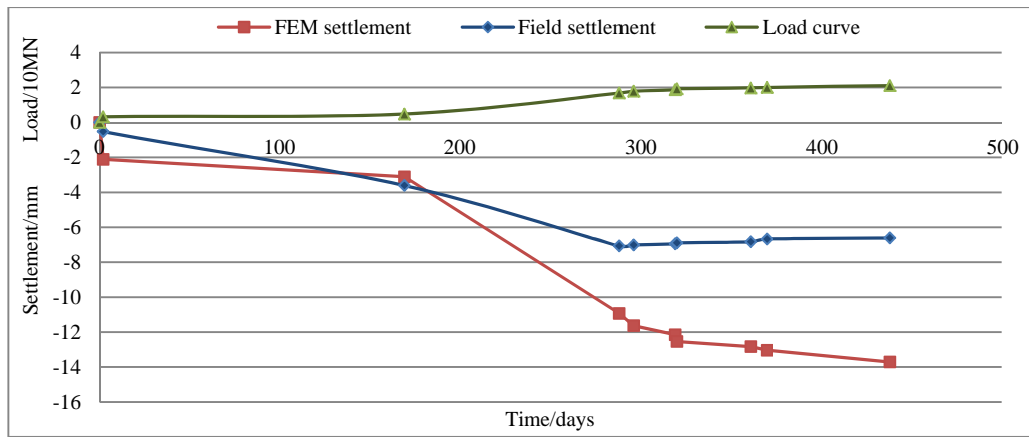


Fig. (32). The calculated results compared with the measured results of DK124.

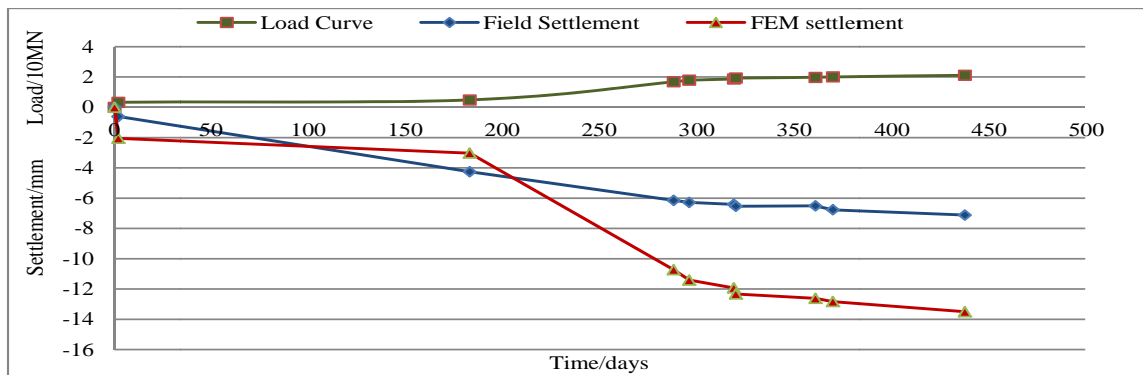


Fig. (33). The calculated results compared with the measured results of DK152.

considered a difficult task in the deep soft soils. The results indicate that the structure would not reach critical settlement values at the completion of consolidation. The predicted settlements being calculated with a statistical regression and a hyperbolic model present corresponding estimates for future settlement. The new method presented in this paper using new empirical equation to calculate the compression modulus in order to predict the settlement in Plaxis 3D program, provides good estimation of the settlement in the deep soft soil area.

The three-dimensional finite element analysis predicts an extent of settlement agreed with that measured on the project site and confirmed the validity of the experimental work. The incremental soil displacements fell within the permissible limits, and the active pore water pressure that indicated the long-term consolidation would not cause excessive settlement after the completion of water dissipation. The total displacement calculated using the modified analysis is 13.71 mm for piers of DK124 and 13.5 mm for piers of DK152.,

They are closely compared to that measured in the field and predicted using the hyperbolic model and statistic regression, which reached a maximum value of 9 mm under the acceptable limit. Therefore, the finite element analysis in Plaxis 3D program with the new modification not only gives a carefully estimation but also an indication of the settlement conditions at the site.

ACKNOWLEDGEMENT

A great thanks to the team of the Beijing Shanghai project for their support and great effort to complete this project. The good and careful suggestions by Professor Dr. Jianlin Ma, the head of Geotechnical department of Southwest Jiaotong University, are also gratefully acknowledged.

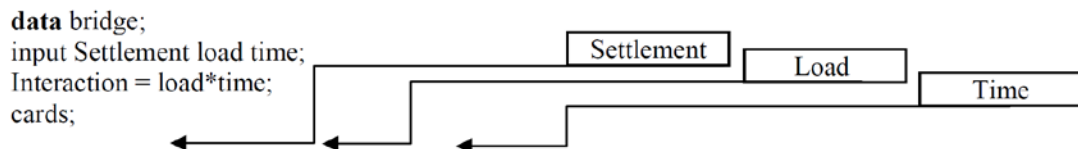
CONFLICT OF INTEREST

The authors confirm that this article content has no conflicts of interest.

APPENDIX A

Code file of settlement data for pier D18

input Settlement load time;



ODS GRAPHICS ON;

PROC univariate Data = bridge;

qqplot settlement; run;

PROC Reg Data = bridge; model Settlement = load time Interaction;

plot predicted.*residual.; run; PROC Reg Data = bridge; model Settlement = time; run;

APPENDIX B

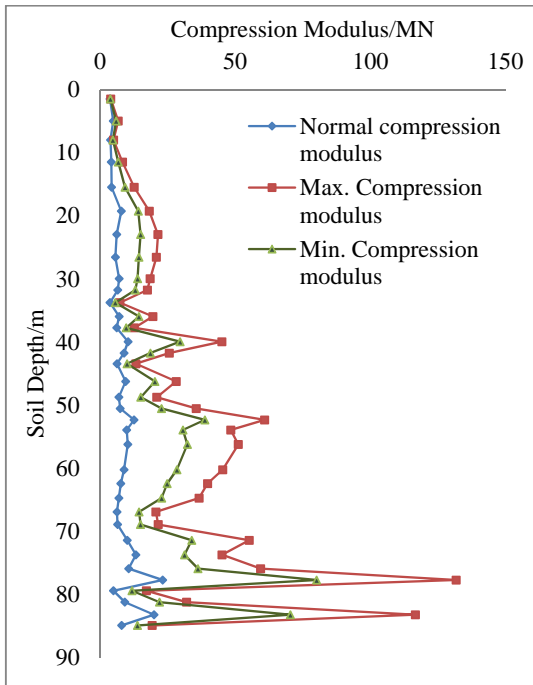


Fig. (B.1). Compression modulus calculation of DK124+676.89.

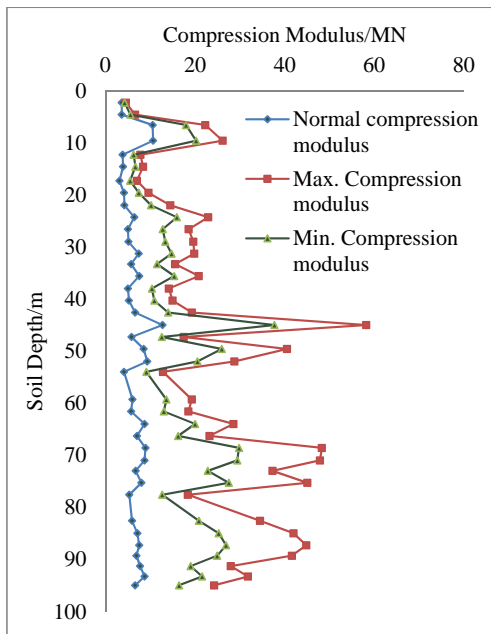


Fig. (B.2). Compression modulus calculation of DK124-644.

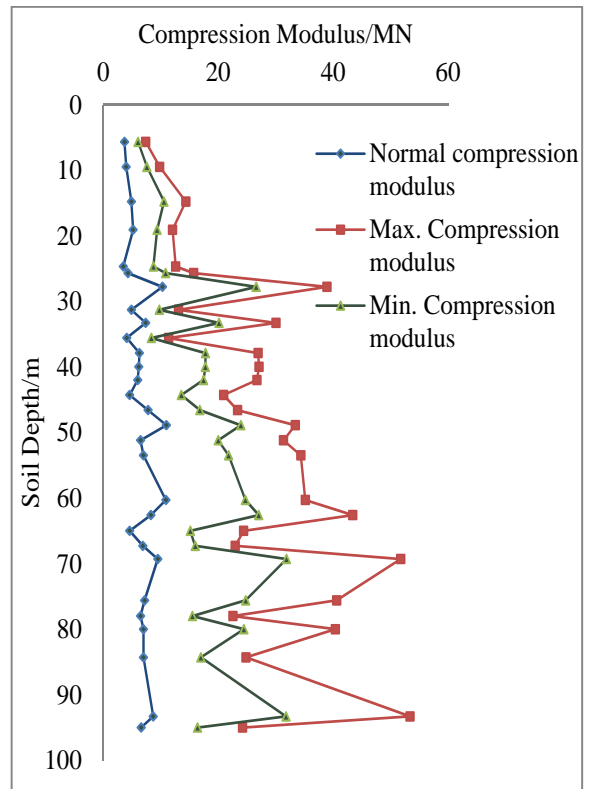


Fig. (B.3). Compression modulus calculation of DK124-710.

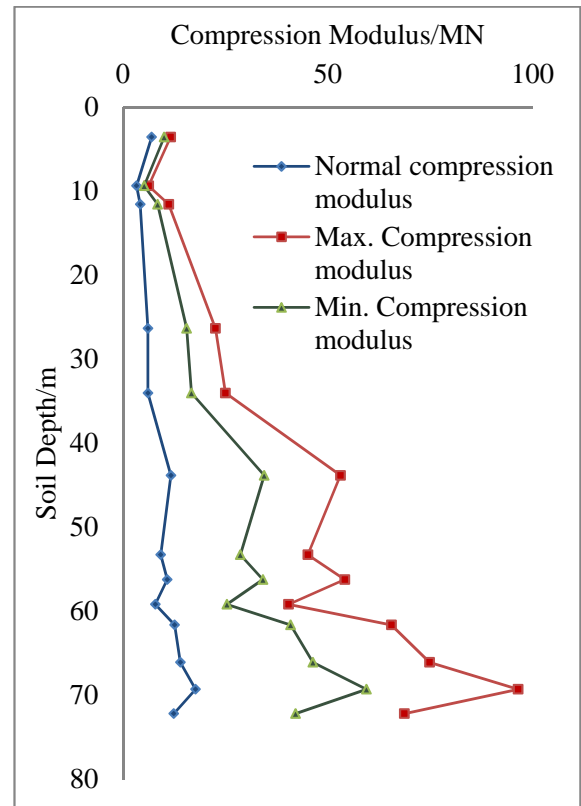


Fig. (B.4). Compression modulus calculation of DK152+996.45. 710.

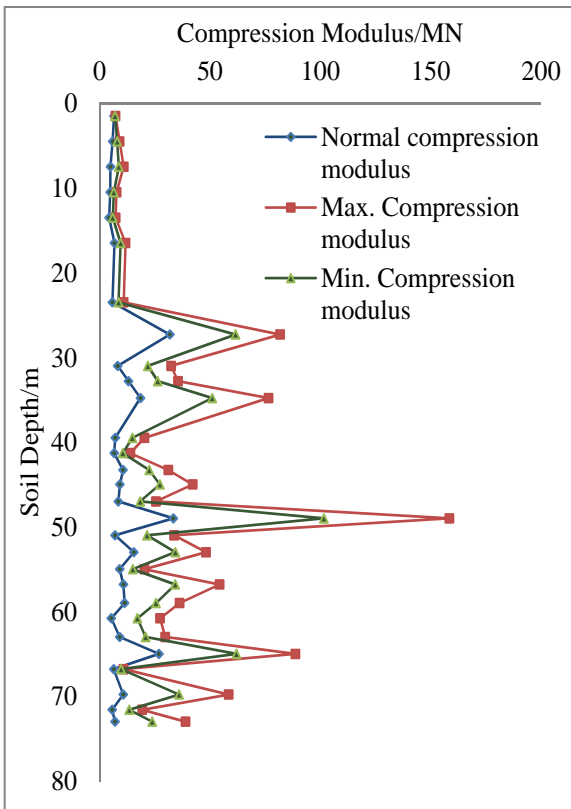


Fig. (B.5). Compression modulus calculation of DK152+981.27.

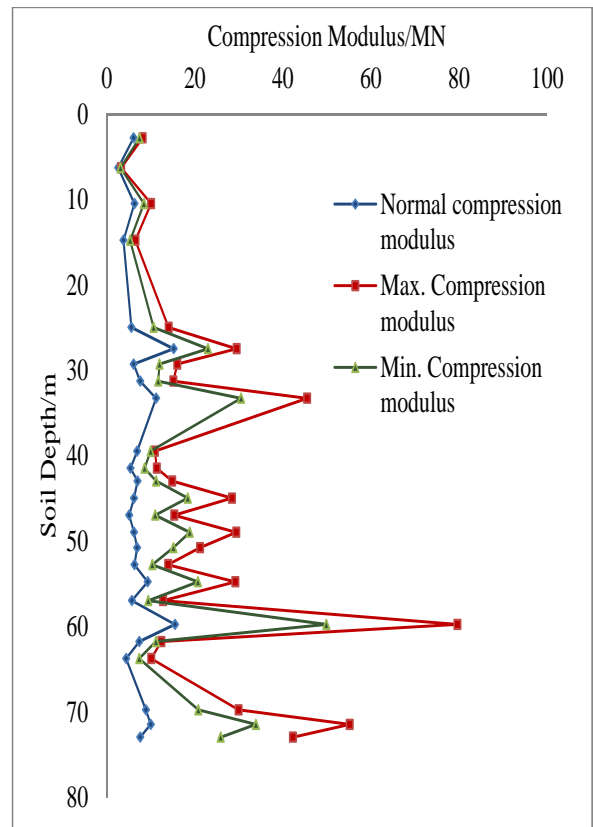


Fig. (B.7). Compression modulus calculation using the new modified formula of DK153+046.67.

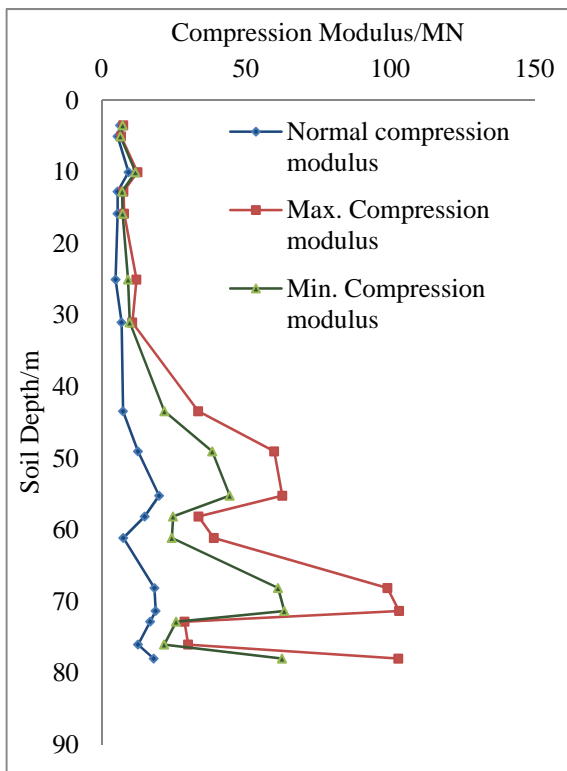


Fig. (B.6). Compression modulus calculation of DK153+013.97.

APPENDIX C

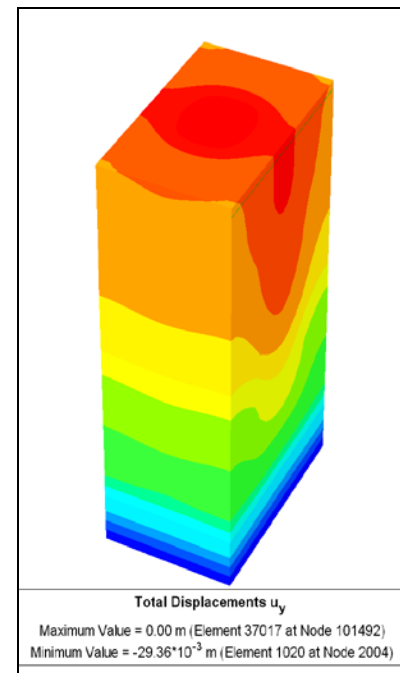


Fig. (C.1). Total vertical displacement (U_y) for soil layers of the DK124 model.

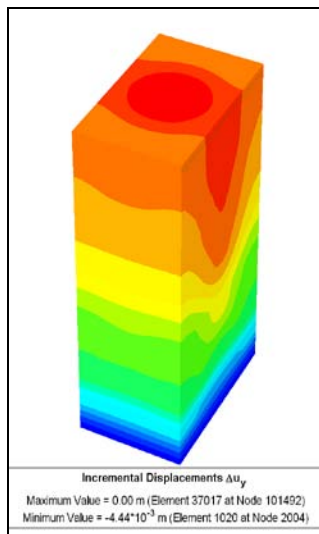


Fig. (C.2). Incremental displacement for soil layers of the DK124 model.

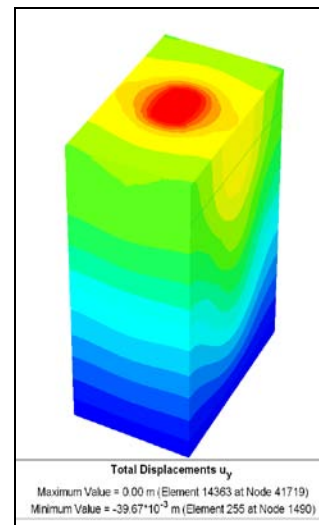


Fig. (C.5). Total vertical displacement (U_y) for soil layers of the DK152 model.

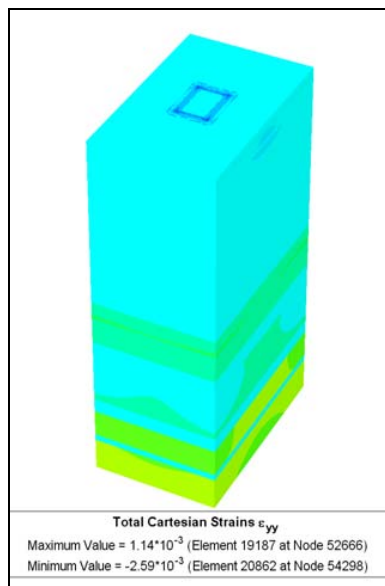


Fig. (C.3). Cartesian total strain for soil layers of the DK124 model.

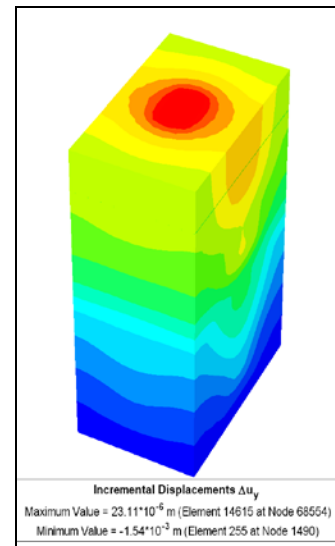


Fig. (C.6). Incremental displacement for soil layers of the DK152 model.

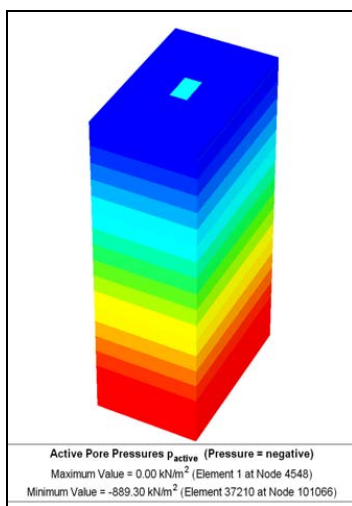


Fig. (C.4). Active pore pressure for soil layers of the DK124 model.

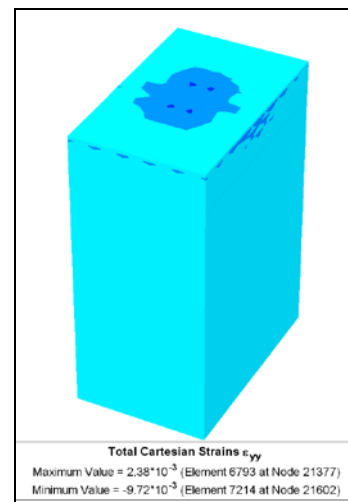


Fig. (C.7). Cartesian total strain for soil layers of the DK152 model.

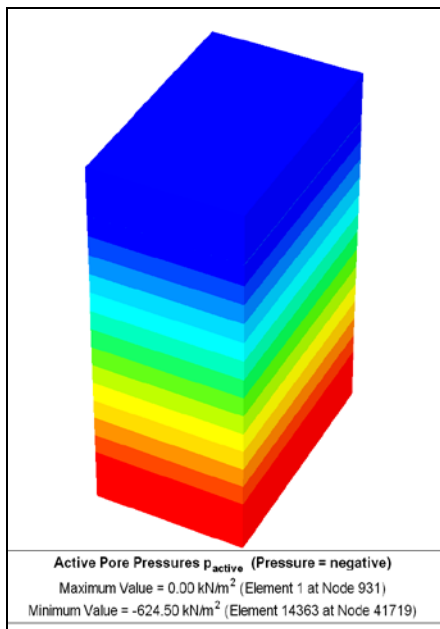


Fig. (C.8). Active pore pressure for soil layers of the DK152 model.

REFERENCES

- [1] C. Zhi-jian, Zhang, N-N Zhang, and X-W Zhang, "Settlement monitoring system of pile-group foundation", *J. Cent. South Univ. Technol.*, vol. 18, pp. 2122-2130, 2011.
- [2] R. Gao, N. Hu, and B. Zhu, "Experimental study and numerical analysis on bearing behaviors of super-long rock-socketed bored pile groups [J]", *J. Southeast Univ.*, vol. 26 no. 4, pp. 597-602, 2010.
- [3] K. Danno and M. Kimura, "Evaluation of long-term displacements of pile foundation using coupled FEM and centrifuge model test", *Soil Found.*, vol. 49, no. 6, pp. 941-958, 2009.
- [4] M. F. Randolph, and C. P. Worth, "Analysis of deformation of vertically loaded piles", *J. Geotech. Eng., ASCE*, vol. 104, no. GT12, pp. 1465-1488, 1978.
- [5] H. G. Poulos, and E. H. Davis, *Pile foundation analysis and design*, UK: John Wiley, 1980.
- [6] C. S. Desai, "Numerical design-analysis for piles in sands" *ASCE*, vol. 100, no. GT6, pp. 613-635, 1974.
- [7] L. Xiaoyan, C. Zhijian, J. Chen, and R. Huaining, "Study on settlement of pile foundation of Sutong Bridge", *2011 International conference on electric technology and civil engineering, ICETCE 2011 - proceedings*, 2011, pp. 772-775.
- [8] G. R. McDowell and M. D. Bolton, "Micro Mechanics of Elastic Soil", *Soil Found.*, vol. 41, no. 6, pp. 147-152, 2001.
- [9] K. M. Lee and Z.R. Xiao "A simplified nonlinear approach for pile group settlement analysis in multilayered soils", *Can. Geotech. J.*, vol. 38, no. 5, pp. 1063-1080, 2001.
- [10] J. G. Bentler and M. J. L. Hoppe, "SCPT for design of shallow bridge foundations in Minnesota", *Am. Eng. Testing, Inc.*, St. Paul, Minnesota, USA, 2009.
- [11] TB 10002.5-2005/ J 464, "Code for Design on Subsoil and Foundation of Railway Bridge and Culvert" [S], 2005, pp. 25-102.
- [12] Republic of China Ministry of Railways, "A total of 200 kilometer per hour passenger railway interim design provisions code", 2007.
- [13] E. C. Hambly, *Bridge deck behavior*, 25, 2nd ed., UK: Taylor and Francis, 1991.
- [14] A. Zolfaghari and M. A. Hajabbasi, "Effect of different land use treatments on soil structural quality and relations with fractal dimensions", *Int. J. Soil Sci.* vol. 3, pp.101-108, 2008.
- [15] G. Leucci, "Integrated geophysical, geological and geomorphological surveys to study the coastal erosion", *Int. J. Soil Sci.*, vol. 1, pp. 146-167, 2006.
- [16] M. L. Leonard, Sr., and K. J. Floom, Jr., "Estimating Method and Use of Landfill Settlement", *Proceedings of Sessions of Geo-Denver ASCE, Environ. Geotech.*, 10.1061/40519 (293)1, 2000.
- [17] S. W. Tan, "Hyperbolic method for prediction of ultimate primary settlement of clays treated with vertical drains", *Compression and consolidation of clayey soils*, Yoshikuni & Kusakabe Eds, The Netherland: Balkema, pp. 795-800, 1995.
- [18] Matyas E. L and Leo Rothenburg. "Estimation of total settlement of embankments by field measurements", *Can. Geotech. J.*, vol. 33, pp. 834-841, 1996.
- [19] H. J. Gibbs, "Estimating Foundation Settlement By One-Dimensional Consolidation Tests". Engineering Laboratories Branch Design and Construction Division, United States Department of the Interior, Bureau of Reclamation, 1953.
- [20] M. A. Al-Shamrani, "Applying the hyperbolic method and Ca/Cc concept for settlement prediction of complex organic-rich soil formations", *Eng. Geol.*, vol. 77, pp. 17-34, 2004.
- [21] Y. Young-Jong and J. Hak-Young, SLC, "Long-term Settlement Prediction of SUDOKWON Landfill site". Gwon Seoung-Hoon, Tescom Engineering co., 2010.
- [22] M. E. F. A El-Salam, "An efficient estimation procedure for determining ridge regression parameter". *Asian J. Math. Stat.*, vol. 4, pp. 90-97, 2011.
- [23] O. E. Okereke, "Some consequences of adding a constant to a least one of the variables in the simple linear regression model". *Asian J. Math. Stat.*, vol. 4, pp. 181-185, 2011.
- [24] M. R. Spiegel, J. J. Schiller and R. A. Srinivasan, "Schaum's outline of theory and problems of probability and statistics". 2nd Ed., New Delhi, India: Tata McGraw-Hill Publishing Company Limited 2000, p: 408.
- [25] L. D. Delwiche, and S. J. Slaughter. "The Little SAS Book": A Primer, 4th ed. Cary, NC: SAS Institute Inc. 2008.
- [26] M. Trochanis, J. Bielak and P. Christiano, "Simplified model for analysis of one or two pile", *J. Geotech. Eng., ASCE*, vol. 117, no. 3, pp. 448-465, 1991.
- [27] M. Trochanis, J. Bielak, and P. Christiano, "Three dimensional nonlinear study of piles", *J. Geotech. Eng., ASCE.*, vol. 117, no. 3, pp. 429-447, 1991.
- [28] K. Terzaghi, R. B. Peck and G. Mesri, "Soil Mechanics in Engineering Practice", 3rd ed., UK: John Wiley & Sons, p.167, 1996.
- [29] F. Farokhzad and A. J. Choobbasti, "Assessing the load size effect in the soil (under single foundation) using finite element method", *Int. J. Soil Sci.*, vol. 3, pp. 209-216, 2011.
- [30] R. Ziaie-Moayed, M. Kamalzare, and M. Safavian, "Evaluation of piled raft foundation behaviour with different dimensions of piles", *J. Appl. Sci.*, vol. 10, pp. 1320-1325, 2010.
- [31] M. Jesmani, M. R. Shafie, and R. S. Vileh, "Three dimensional analysis of active isolation of deep foundations by open rectangular trenches", *J. Appl. Sci.*, vol. 14, pp. 2544-2555, 2009.
- [32] British Standard 5930:1999, University of Sheffield, Uncontrolled Copy, (c) BSI, 2004, pp. 122.
- [33] V. Bakholdin and L. P. Chashchikhina, "Determination of the compression modulus of soils from compression-test data for calculation of pile-foundation settlements", *Soil Mech. Found. Eng.*, vol. 36, no. 1, pp. 9-12, DOI: 10.1007/BF02471292, 1999.
- [34] M. A. Al-Naeem, "Influence of water stress on water use efficiency and dry-hay production of alfalfa in Al-Ahsa", *Saudi Arabia. Int. J. Soil Sci.*, vol. 3, pp. 119-126, 2008.